Biochemistry and Biophysics Reports 15 (2018) 7–12

Contents lists available at ScienceDirect

Biochemistry and Biophysics Reports

journal homepage: www.elsevier.com/locate/bbrep

In vitro interactions of histones and α-crystallin

Paul D. Hamilton, Usha P. Andley*

Department of Ophthalmology and Visual Sciences, Washington University School of Medicine, St. Louis, MO, USA

ARTICLE INFO

Keywords:
Histone
Complex formation
Cataract
Crystallin

ABSTRACT

The aggregation of crystallins in lenses is associated with cataract formation. We previously reported that mutant crystallins are associated with an increased abundance of histones in knock-in and knockout mouse models. However, very little is known about the specific interactions between lens crystallins and histones. Here, we performed *in vitro* analyses to determine whether α-crystallin interacts with histones directly. Isothermal titration calorimetry revealed a strong histone–α-crystallin binding with a K_d of 4×10^{-7} M, and the thermodynamic parameters suggested that the interaction was both entropy and enthalpy driven. Size-exclusion chromatography further showed that histone–α-crystallin complexes are water soluble but become water insoluble as the concentration of histones is increased. Right-angle light scattering measurements of the water-soluble fractions of histone–α-crystallin mixtures showed a decrease in the oligomeric molecular weight of α-crystallin, indicating that histones alter the oligomerization of α-crystallin. Taken together, these findings reveal for the first time that histones interact with and affect the solubility and aggregation of α-crystallin, indicating that the interaction between α-crystallin and histones in the lens is functionally important.

1. Introduction

α-Crystallin is a major protein of mammalian lenses and is essential for lens transparency. Crystallin aggregation in cataracts in humans is associated with aging, environmental UV stress, and genetic mutations [1–3]. Point mutations in crystallin genes that have been associated with cataracts have been introduced in mouse models to investigate the mechanism of cataractogenesis *in vivo* [4,5].

We previously demonstrated that lens epithelial cells expressing the R116C mutation in αA-crystallin have increased abundances of histones H2B and H4 [6]. Similarly, proteomics analyses on the lenses of *Cryaa*-R49C knock-in mice and young *Cryaa/Cryab* double knockout mice show increases in H2B and H4 as well as H2A [7,8]. Other recent studies also suggest that α-crystallin has a functional relationship with histones, though very little is known about the specific role of histones in the lens [9,10]. In yeast cells, the upregulation of histones was shown to improve cell survival [11]. Although histones can be found in the cell cytoplasm and extracellular space and are involved in inflammation, cancer, and other pathologies [12], their primary function is in the nucleus, where they package DNA into nucleosomes—the basic building blocks of chromatin—and are involved in transcriptional regulation [13–15]. An increase in histones in lenses from the αA-R49C mutant mice may be indicative of an increase in nucleosome density, and a functional increase in the histone/DNA ratio may lead to increased amounts of heterochromatin. The increase in histone transcripts in *Cryaa*-R49C mice suggests that the increase in gene expression of histones may be an early event in cataractogenesis, though the notion that α-crystallin functions as a modulator of the expression of histones has not yet been investigated [16]. Nevertheless, these findings strongly suggest a functional relationship between histones and α-crystallin.

We also discovered that the mutant αA-R49C protein is distributed mainly in the nuclei of transfected lens epithelial cells, where it may bind and sequester histones [17]. Indeed, our proteomic analyses revealed that α-crystallin and histones are colocalized in cataractous lenses [7,8]. As a negatively charged protein, α-crystallin may directly bind to histones, but this possibility has not been tested *in vitro*. It also remains unclear whether α-crystallin exists as a stable complex with histones or serves as a transcriptional inhibitor.

Many chaperones such as Nasp, Npm2 and Asf1 are involved in the sequestration, import, and deposition of histones onto chromatin [18–23]. Histone chaperones are known to bind histones and shield them from non-specific interactions [24]. Additionally, mouse erythroblasts transfer histones and non-histone proteins from the nucleus to the cytoplasm, and a similar process may occur in denucleating lens fiber cells *in vivo* [25]. Investigation of an *in vitro* interaction between histones and α-crystallin may thus provide insight into their functional

Abbreviations: GPC, gel permeation chromatography; HS, high salt; ITC, isothermal titration calorimetry; MALDI-TOF MS, matrix-assisted laser-desorption/ionization-time of flight mass spectrometry; PBS, phosphate-buffered saline; RALS, right-angle light scattering

* Correspondence to: Department of Ophthalmology and Visual Sciences, Washington University School of Medicine, 660 South Euclid Avenue, Campus Box 8096, St. Louis, MO, USA.
E-mail address: andley@wustl.edu (U.P. Andley).

https://doi.org/10.1016/j.bbrep.2018.05.005
Received 12 April 2018; Received in revised form 15 May 2018; Accepted 17 May 2018
Available online 01 June 2018

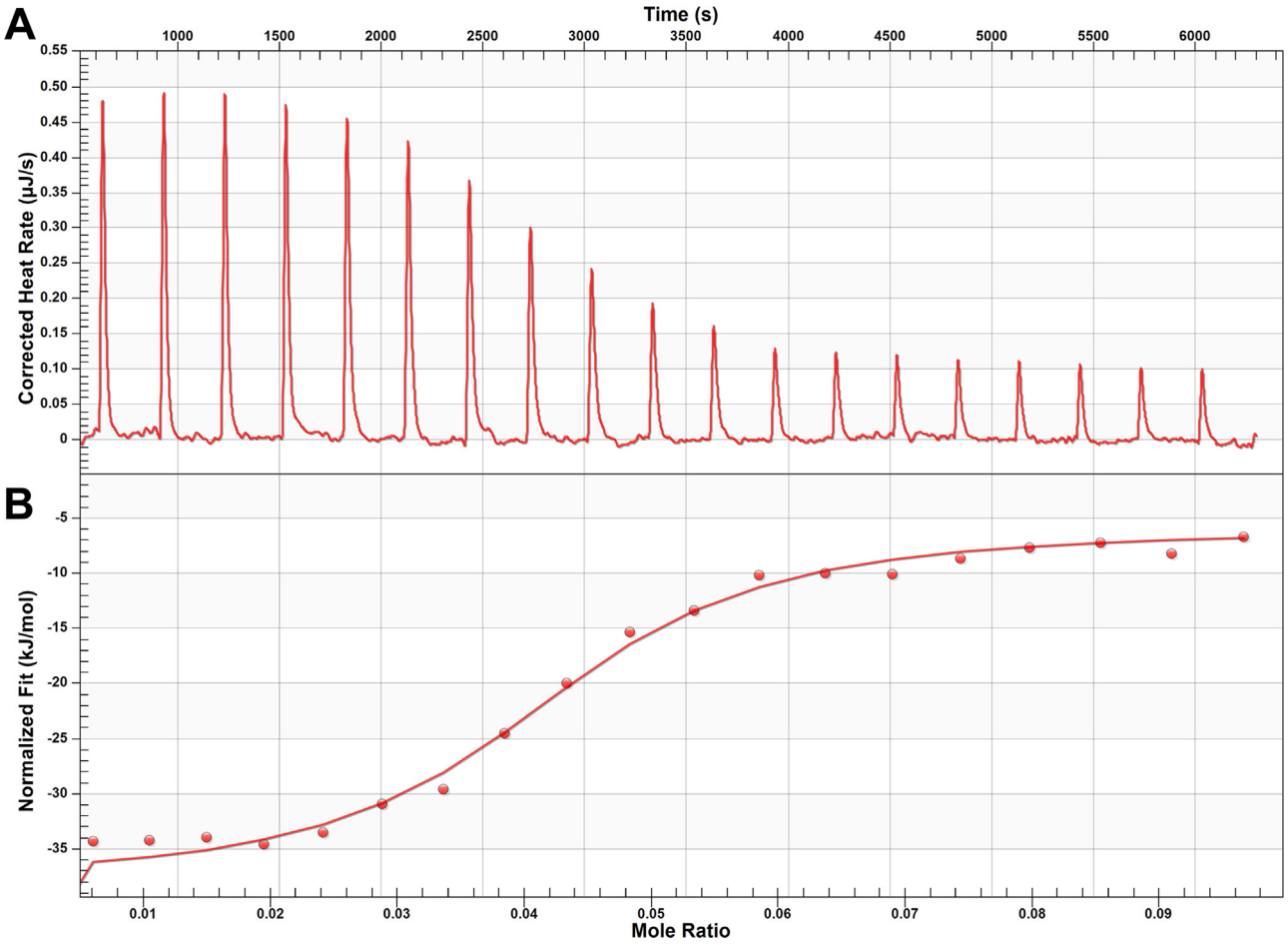

Fig. 1. Isothermal titration calorimetric (ITC) analysis of the interaction between histones and α-crystallin. (A) Changes in current were recorded after sequential injections of 150 µM α-crystallin into a solution of histones (514 µM). (B) Integrated and normalized areas under each peak were plotted against the mole ratio (α-crystallin/histone); the red line shows the fit of the data using the NanoAnalyze program.

Table 1
Thermodynamic parameters of α-, βH, βL-, and γ-crystallin binding to histones.

Sample[a]	K_d	n	ΔH (kJ/mol)	ΔS (J/mol K)	ΔG (kJ/mol)	− TΔS (kJ/mol)	K_a (M^{-1})
α-Crystallin	4.00E−7	0.042	− 26.32	34.20	− 36.52	− 10.20	2.50E6
α-Crystallin HS	2.93E−8	0.040	− 7.60	118.7	− 43.00	− 35.40	3.42E7
βL-Crystallin	8.64E−8	0.036	− 44.80	− 15.05	− 40.32	4.49	1.15E7
βL-Crystallin HS	7.43E−7	0.021	− 37.07	− 6.99	− 34.98	2.08	1.35e6
γ-Crystallin	1.27E−7	0.035	− 55.92	− 55.54	− 39.36	16.56	7.85E6
γ-Crystallin HS	1.02E7	0.010	−65.91	−87.22	−39.90	26.00	9.79E6

[a] Sample concentrations were 150 µM (3 mg/ml) α- or γ-crystallin or 120 µM (3 mg/ml) βL-crystallin with 514 µM (7.2 mg/ml) histones (predissolved for 6 h). HS refers to 0.5 M NaCl-containing phosphate-buffered saline (PBS).

relationship *in vivo*. Therefore, we performed isothermal titration calorimetry (ITC), as well as size-exclusion chromatography and gel electrophoresis, to investigate histone–α-crystallin interactions *in vitro*. The results from this study provide information from which we can design new experiments to better understand the role of histone–α-crystallin interactions in eye tissues and pathologies.

2. Materials and methods

2.1. ITC

Protein–protein interactions between histones and α-crystallin were examined on a nano-ITC instrument (TA Instruments). Histones (bovine) were obtained from Sigma-Aldrich (catalog number H9250) and crystallin proteins (α-, βH-, βL- and γ-crystallin) were purified from porcine lenses [26]; protein solutions were prepared in phosphate-buffered saline (PBS). Preliminary experiments indicated that the time for which the histones were dissolved in PBS was relevant; however, allowing the histones to dissolve in solution for 3 h reduced this effect. MALDI-TOF MS analysis of histones obtained from Sigma showed that this preparation contains the core histones H2a, H2b, H3 and H4 histones (Supplementary Fig. S1).

The ITC instrument was validated using a nano-ITC validation kit according to the manufacturer's instructions. The reference cell was washed three times and then filled with 300 µl deionized and degassed water. The calorimeter was equilibrated to a baseline drift of less than 100 nW over 10 min. Next, the sample cell was washed three times and filled with the histone solution. Twenty sequential injections of 2.50 µl α-crystallin were then made at room temperature (25 °C) with a stirring speed of 350 rpm; the processes for titrating βH-, βL-, and γ-crystallins

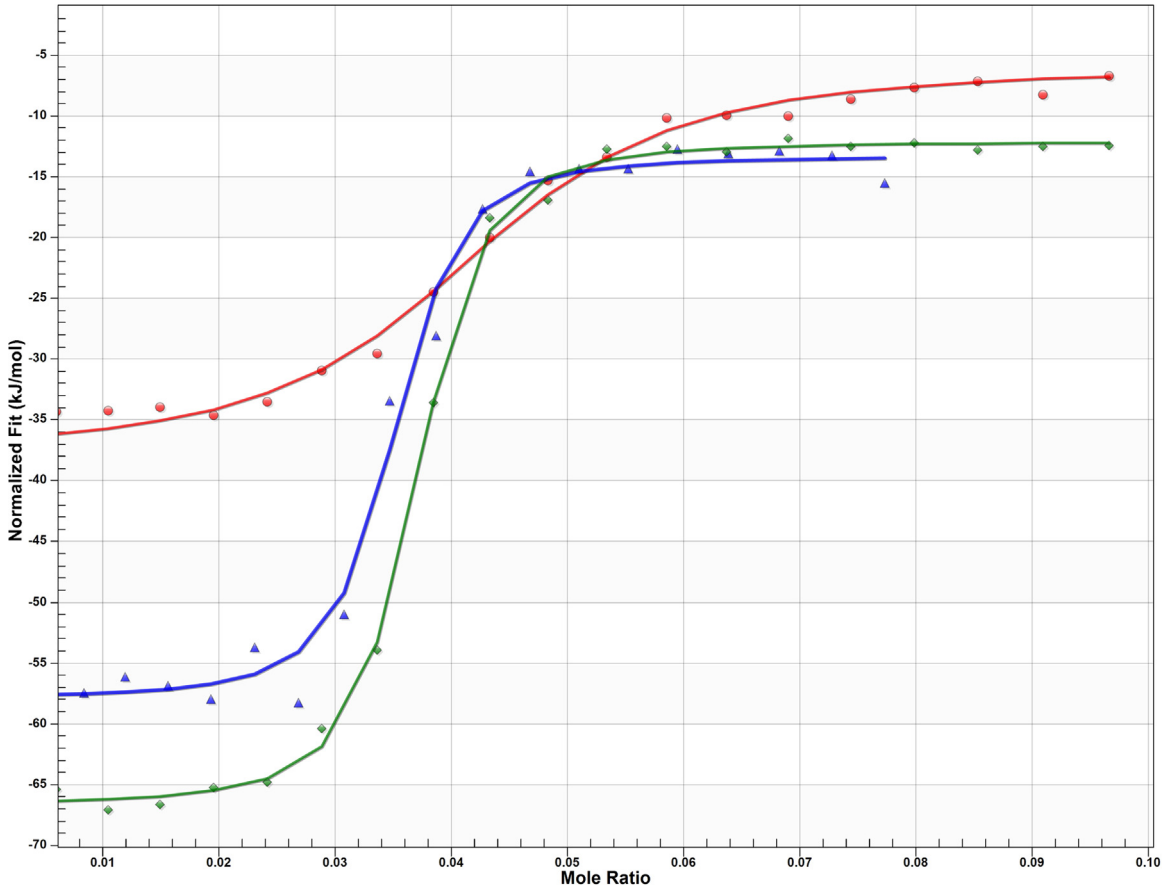

Fig. 2. Isothermal titration calorimetric (ITC) analysis of the interaction between histones and βL-crystallin or γ-crystallin. Changes in current were recorded after sequential injections of 150 μM βL-crystallin (blue) or γ-crystallin (green) into a solution of histones (514 μM); data for α-crystallin are shown in red for comparison.

were similar. We first performed preliminary experiments with equal concentrations (mg/ml) of α-crystallin and histones, and then tested other concentrations to get the mid-point of the interaction curve. The ITC software provides the optimal concentrations of the proteins to use to obtain the interaction data. The optimal concentration ratio of crystallins to histones, which was determined in preliminary studies, was 150 μM (3 mg/ml) α-crystallin to 514 μM (7.2 mg/ml) histones in the presence of 1 mM ATP. To calculate molar concentrations of crystallins and histones, we used the subunit molecular masses of 20 kDa (25 kDa for βL-crystallin) and 14 kDa, respectively. The binding of α-crystallin to histones was examined at 3, 6, and 24 h after the preparation of the histone solution. The interactions between histones and crystallins were also examined at high salt concentrations in PBS containing 0.5 M NaCl. Additionally, control ITC titrations were done in the absence of ATP or histones.

The titration data were analyzed using NanoAnalyze software (TA Instruments) in which the upward peaks correspond to an exothermic reaction. The heat of dilution resulting from injecting the protein into the buffer was determined and subtracted before data fitting. The enthalpy (ΔH), dissociation constant (K_d), and stoichiometry of the interaction (n) were calculated using the heat changes directly measured between α-crystallin and histones. The entropy (ΔS) and binding free energy (ΔG) of the interaction were calculated with the NanoAnalyze software.

2.2. GPC

α-Crystallin (50 μM) was incubated with increasing concentrations of histones: 0.0714, 0.143, 0.357, 0.536, 0.714, 1.071, 1.43, 1.79, and 2.14 μM (1, 2, 5, 7.5, 10, 15, 20, 25, and 30 μg/ml, respectively). The histone–α-crystallin mixtures were then filtered through 0.22-μm filters and water-soluble proteins were separated in succession on G3000 PWXL and G5000 PWXL size-exclusion chromatography columns (Tosoh Bioscience LLC, Prussia, PA) in line with the Viscotek TDA 302 triple-detector array system (Viscotek/Malvern) equipped with a VE-1122 pump and a VE-7510 degasser for measuring UV absorption, refractive index, right-angle light scattering (RALS), and viscosity. Viscotek OmniSEC software was used to calculate the molecular weights of the crystallin proteins using bovine serum albumin and the 92-kDa Pullulan Malvern standards. The protein samples (100 μl) were injected into the columns with 0.5× Dulbecco's modified PBS as the mobile phase at a flow rate of 0.8 ml/min at 37 °C. The protein concentrations were calculated on the basis of the refractive index using a *dn/dc* of 0.185 for both the bovine serum albumin standard and the crystallin proteins.

2.2.1. Gel electrophoresis

Supernatants and pellets were obtained by centrifuging (10,000 rpm for 30 min) the complexes of α-crystallin (50 μM) and histones (0.4–6.42 μM) after a 1-h incubation at 37 °C. Thirty microliters of electrophoresis sample buffer (Novex LC2676 Tris-glycine-SDS buffer; Life Technologies) was added to each pellet, and 20 μl was added to the lanes of 10–20% Tris-glycine gels (Life Technologies). Prestained molecular weight markers (Invitrogen) were used on all gels. After the electrophoresis, the gels were stained with Coomassie blue or transferred to polyvinylidene difluoride membranes and stained with Revert protein stain (LI-COR Biosciences, Lincoln, NE, USA) and visualized on an Odyssey analyzer (LI-COR).

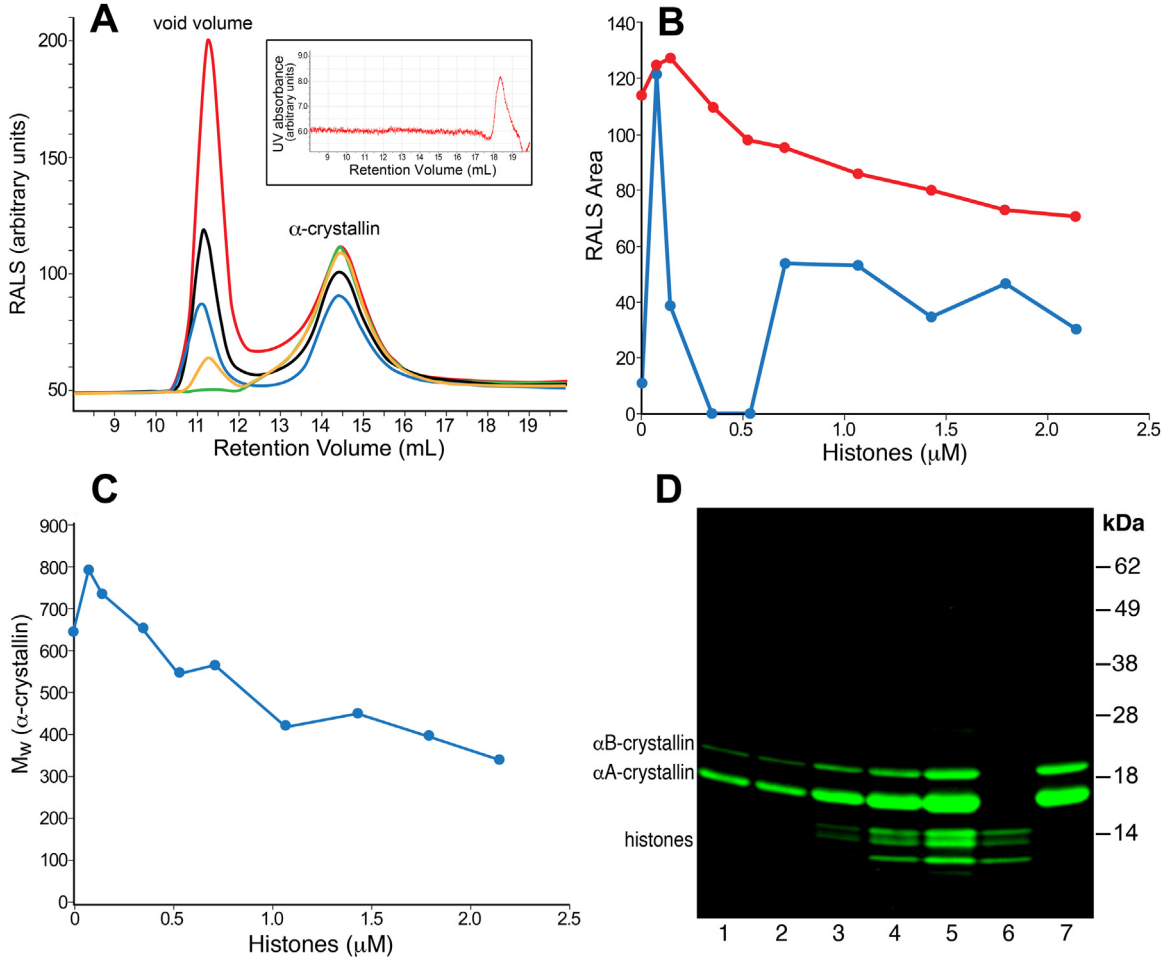

Fig. 3. GPC of α-crystallin incubated with histones. α-Crystallin (50 μM; 1 mg/ml) was incubated with increasing concentrations of histones. (A) Right-angle light scattering (RALS) of the soluble proteins in the filtered samples. The void volume peak represents the high-molecular-weight water-soluble proteins and the α-crystallin peak represents the normal α-crystallin in the samples incubated with histones at concentrations of 0 μM (yellow), 0.0714 μM (red), 0.357 μM (green), 1.071 μM (black), or 2.14 μM (blue). The inset shows the UV absorbance (218 nm) of histones only. (B) Integration areas of the peak areas of the void volume (blue) and α-crystallin (red) at different histone concentrations. Note that the two points on the x-axis represent histone concentrations where the water-soluble high-molecular-weight peak is negligible. At 0.357 μM histone, α-crystallin does aggregate but the aggregate was too large to remain in the water-soluble fraction and became water insoluble. (C) Molecular weights of the α-crystallin peaks calculated from RALS at different histone concentrations. (D) Revert protein-stained polyvinylidene difluoride membrane following sodium dodecyl sulfate polyacrylamide gel electrophoresis (SDS-PAGE) of the water insoluble fractions from mixtures of 50 μM α-crystallin and various histone concentrations: lane 1, 0.429 μM; lane 2, 0.1.07 μM; lane 3, 2.14 μM; lane 4, 4.28 μM; lane 5, 6.42 μM, lane 6, 6.42 μM histones without α-crystallin; and lane 7, 50 μM α-crystallin without histones.

3. Results and discussion

3.1. Interaction of histones with α-crystallin by ITC

As previous studies indicated that α-crystallin functionally interacts with histones *in vivo*, observed as increases in histone–α-crystallin-complexes and transcripts in *Cryaa/Cryab* knockout mice and in mouse lenses expressing a mutant α-crystallin [6–8,16], we sought to verify this *in vitro*. The results from ITC experiments revealed that an interaction occurs in mixtures of 150 μM α-crystallin and 514 μM histones (Fig. 1A). Fig. 1B shows the integrated and normalized area under each peak plotted against the mole ratio (α-crystallin/histone); the curve fitting (red line) was determined by the NanoAnalyze program. The titrations also showed that the binding of α-crystallins and histones is exothermic with favorable binding enthalpy and entropy (Table 1). The negative enthalpy (ΔH) values show a high selectivity of the direct or specific interactions between histones and α-crystallin [27], whereas the entropy (ΔS value) is usually related to solvation effects [27]. The K_d value indicates that the binding between histones and α-crystallin occurs with high affinity. The stoichiometry of histone and α-crystallin binding suggests that it involves more than a charge interaction between the acidic groups of α-crystallin and basic groups, such as lysines, on histones. Indeed, the binding interactions were not substantially altered under a high salt condition (Table 1), indicating that ionic interactions do not have a primary role in their association. Thus, the binding may be due to hydrophobic interactions. Association of histone with α-crystallin was ATP-dependent (Supplemental Fig. S2). ATP has been shown to affect the structure of the core domain of αB-crystallin [28]. ITC titrations in the absence of ATP showed no significant interaction between histones and α-crystallin.

As mammalian lenses express high concentrations of βH, βL-, and γ-crystallins as well as α-crystallin, we also assessed their interactions with histones *in vitro*. Unexpectedly, βH-crystallin did not exhibit any appreciable interaction with histones by ITC analysis; however, the βL- and γ-crystallins displayed strong interactions with histones, as indicated by the dissociation constants (Fig. 2 and Table 1). However, unlike histone–α-crystallin complexes, we did not observe precipitation of the histone–βL-crystallin and histone–γ-crystallin mixtures. The interaction of βL- or γ-crystallins with histones had a favorable large binding enthalpy (negative ΔH values) that exceeded the unfavorable

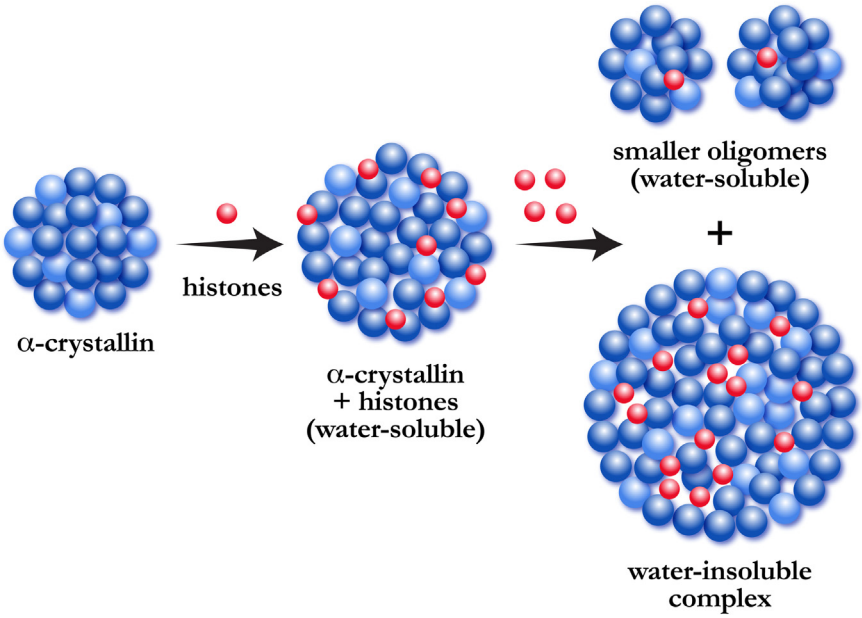

Fig. 4. Schematic model depicting the effects of histones (red circles) on the aggregate size and solubility of α-crystallin (blue circles). At low histone/α-crystallin ratios, a high-molecular-weight water-soluble complex is formed (middle panel). As the histone concentration increases, the proteins form larger water insoluble aggregates that cannot be detected in the GPC analysis of the supernatants (Fig. 3B). With a further increase in histone/α-crystallin ratios, a mixture of water-soluble and water insoluble complexes is observed (right panel), with a decrease in the oligomeric size in the water-soluble fraction. Note that histones and α-crystallins are not drawn to scale.

binding entropy (negative ΔS), suggesting that these interactions are enthalpy driven. The unfavorable ΔS values suggest that water solvates the histone-binding regions of βL- and γ-crystallins, leading to more hydrogen bonding and ionic interactions than in the case of α-crystallin (where water molecules may be extruded from the binding region) and the configurationally unfavorable entropy (entropy penalty) (Table 1) [27]. Notably, the ΔG values were nearly identical for the binding of histones with α-, βL-, and γ-crystallins. It should also be noted that the overall binding of histones to α-crystallin was expected to be greater because α-crystallin has more subunits (~ 30) per molecule than βL- and γ-crystallin (2 and 1 subunit, respectively).

The stoichiometry of association of α-crystallin with histones suggests that histones may be forming a complex when bound to α-crystallin. Histones are known to form octamers when bound to DNA [13,14]. Further studies will be necessary to determine whether histones form multimers when bound to α-crystallin. Alternatively, only a limited number of α-crystallin binding sites may be available on histones, and hence a large excess of histones is required to obtain the stoichiometry. This stoichiometry was not affected by a high salt concentration, suggesting that this association was not driven by ionic interactions (Table 1). Similarly, the stoichiometry values of βL- and γ-crystallins had a high number of histones associating with each crystallin. In contrast to α-crystallin, stoichiometric values were reduced further under a high salt condition in the βL- and γ-crystallin (Table 1). For example, γ-crystallin had a 3.5-fold lower n value at a high salt concentration, indicating that the histone–γ-crystallin binding is largely ionic in nature and that the binding sites were blocked by the salt. These data also show that the binding of histones to βL- and γ-crystallins was enthalpy driven, even at high salt concentrations.

3.1.1. *Interaction of histones with α-crystallin by GPC*

We also assessed the histone–α-crystallin interaction *in vitro* by GPC. After mixing α-crystallins with a low concentration of histones (α-crystallin subunit/histone molar ratio of 231), a water-soluble protein aggregate of α-crystallin with a 30% higher molecular weight was observed in the void volume, which may have resulted from a binding interaction between α-crystallin and histones (Fig. 3A). As the histone concentration was increased (α-crystallin subunit/histone molar ratios of up to 2.6), a gradual but continual decrease in the molecular weight of the water-soluble α-crystallin peak was observed, as shown by RALS values (Fig. 3B). Concurrently, the amount of α-crystallin in the water-soluble fraction decreased. Additionally, a pellet was visible in the mixture after centrifugation, indicating that a portion of the histone–α-crystallin complex became water insoluble. An SDS-PAGE analysis of the water insoluble fraction revealed increased protein amounts and detectable histone bands with the addition of higher histone concentrations (Fig. 3D), suggesting the histone–α-crystallin complex became water insoluble. The SDS-PAGE analysis verified that α-crystallin preparations were uncontaminated with β- or γ-crystallins. These results indicate that histones associate with α-crystallin in the large water insoluble aggregates. Furthermore, histones appear to affect the subunit–subunit interactions and aggregation behavior of α-crystallin and cause it to dissociate into lower-molecular-weight water-soluble oligomers (Fig. 3B and C). Whereas the molecular weight of α-crystallin was higher at a low histone/α-crystallin ratio due to the formation of a high-molecular-weight complex, the complex was partially insoluble at higher histone/α-crystallin ratios accompanied by a decrease in the molecular weight of the water-soluble species (Fig. 3A and B). However, unlike histone–α-crystallin complexes, we did not observe precipitation of the histone–βL-crystallin and histone–γ-crystallin mixtures. Fig. 4 shows a proposed model for the effect of histones on α-crystallin oligomerization.

In a previous work with transfected cell lines, we observed a redistribution of mutant α-crystallin into the cell nuclei [17], where histones are primarily confined, suggesting that mutant αA-crystallin may interact with and sequester histones that would otherwise be incorporated into chromatin. α-crystallin may be more amenable to interaction with histones in the cell nucleus of *Cryaa*-R49C cataractous mouse lenses [17]. *In vivo*, these interactions are likely affected by posttranslational histone modifications, such as methylation, acetylation (which neutralizes the positive charge), and phosphorylation (which adds to the negative charge and causes chromatin decondensation). Additional studies of the interactions between modified histones and mutant crystallins are needed to determine which modifications stabilize or promote the interactions between these proteins.

In summary, we demonstrate a strong *in vitro* interaction between histones and α-crystallin using ITC, a method that has not been used previously to study histone–α-crystallin interactions. We found that whereas the binding of histones to α-crystallin was enthalpy and entropy driven, that to βL- and γ-crystallin was enthalpy driven. Moreover, βL- and γ-crystallin binding with histones was dependent on ionic interactions, which were less important for α-crystallin binding. These findings validate those from *in vivo* studies in mouse models of cataracts, which suggest a relationship between histones and crystallins

[8,16].

Acknowledgements

Lens crystallins were a gift from Dr. Nathan Ravi. This work was supported by National Institutes of Health (NIH) grants R01EY05681 (to UPA), NIH Core grant EY02687 and a Research to Prevent Blindness grant to the Department of Ophthalmology and Visual Sciences at Washington University.

Appendix A. Supporting information

Supplementary data associated with this article can be found in the online version at http://dx.doi.org/10.1016/j.bbrep.2018.05.005.

References

[1] H. Bloemendal, W. de Jong, R. Jaenicke, N.H. Lubsen, C. Slingsby, A. Tardieu, Ageing and vision: structure, stability and function of lens crystallins, Prog. Biophys. Mol. Biol. 86 (2004) 407–485.
[2] U.P. Andley, Crystallins and hereditary cataracts: molecular mechanisms and potential for therapy, Expert Rev. Mol. Med. 8 (2006) 1–19.
[3] U.P. Andley, Crystallins in the eye: function and pathology, Prog. Retin Eye Res. 26 (2007) 78–98.
[4] U.P. Andley, P.D. Hamilton, N. Ravi, Mechanism of insolubilization by a single-point mutation in alphaA-crystallin linked with hereditary human cataracts, Biochemistry 47 (2008) 9697–9706.
[5] U.P. Andley, P.D. Hamilton, N. Ravi, C.C. Weihl, A knock-in mouse model for the R120G mutation of alphaB-crystallin recapitulates human hereditary myopathy and cataracts, PLoS One 6 (2011) e17671.
[6] U.P. Andley, H.C. Patel, J.H. Xi, The R116C mutation in alpha A-crystallin diminishes its protective ability against stress-induced lens epithelial cell apoptosis, J. Biol. Chem. 277 (2002) 10178–10186.
[7] U.P. Andley, J.P. Malone, P.D. Hamilton, N. Ravi, R.R. Townsend, Comparative proteomic analysis identifies age-dependent increases in the abundance of specific proteins after deletion of the small heat shock proteins alphaA- and alphaB-crystallin, Biochemistry 52 (2013) 2933–2948.
[8] U.P. Andley, J.P. Malone, R.R. Townsend, In vivo substrates of the lens molecular chaperones alphaA-crystallin and alphaB-crystallin, PLoS One 9 (2014) e95507.
[9] L. Wolf, W. Harrison, J. Huang, Q. Xie, N. Xiao, J. Sun, L. Kong, S.A. Lachke, M.R. Kuracha, V. Govindarajan, P.K. Brindle, R. Ashery-Padan, D.C. Beebe, P.A. Overbeek, A. Cvekl, Histone posttranslational modifications and cell fate determination: lens induction requires the lysine acetyltransferases CBP and p300, Nucleic Acids Res. 41 (2013) 10199–10214.
[10] N. Maki, P.A. Tsonis, K. Agata, Changes in global histone modifications during dedifferentiation in newt lens regeneration, Mol. Vis. 16 (2010) 1893–1897.
[11] J. Feser, D. Truong, C. Das, J.J. Carson, J. Kieft, T. Harkness, J.K. Tyler, Elevated histone expression promotes life span extension, Mol. Cell 39 (2010) 724–735.
[12] R. Chen, R. Kang, X.G. Fan, D. Tang, Release and activity of histone in diseases, Cell Death Dis. 5 (2014) e1370.
[13] B. Li, M. Carey, J.L. Workman, The role of chromatin during transcription, Cell 128 (2007) 707–719.
[14] M.R. Hubner, M.A. Eckersley-Maslin, D.L. Spector, Chromatin organization and transcriptional regulation, Curr. Opin. Genet. Dev. 23 (2013) 89–95.
[15] T. Kouzarides, Chromatin modifications and their function, Cell 128 (2007) 693–705.
[16] U.P. Andley, E. Tycksen, B.N. McGlasson-Naumann, P.D. Hamilton, Probing the changes in gene expression due to alpha-crystallin mutations in mouse models of hereditary human cataract, PLoS One 13 (2018) e0190817.
[17] D.S. Mackay, U.P. Andley, A. Shiels, Cell death triggered by a novel mutation in the alphaA-crystallin gene underlies autosomal dominant cataract linked to chromosome 21q, Eur. J. Hum. Genet. 11 (2003) 784–793.
[18] A.J. Andrews, G. Downing, K. Brown, Y.J. Park, K. Luger, A thermodynamic model for Nap1-histone interactions, J. Biol. Chem. 283 (2008) 32412–32418.
[19] R.J. Burgess, Z. Zhang, Histone chaperones in nucleosome assembly and human disease, Nat. Struct. Mol. Biol. 20 (2013) 14–22.
[20] M. Hondele, T. Stuwe, M. Hassler, F. Halbach, A. Bowman, E.T. Zhang, B. Nijmeijer, C. Kotthoff, V. Rybin, S. Amlacher, E. Hurt, A.G. Ladurner, Structural basis of histone H2A-H2B recognition by the essential chaperone FACT, Nature 499 (2013) 111–114.
[21] M.C. Ho, C. Wilczek, J.B. Bonanno, L. Xing, J. Seznec, T. Matsui, L.G. Carter, T. Onikubo, P.R. Kumar, M.K. Chan, M. Brenowitz, R.H. Cheng, U. Reimer, S.C. Almo, D. Shechter, Structure of the arginine methyltransferase PRMT5-MEP50 reveals a mechanism for substrate specificity, PLoS One 8 (2013) e57008.
[22] B.G. Kuryan, J. Kim, N.N. Tran, S.R. Lombardo, S. Venkatesh, J.L. Workman, M. Carey, Histone density is maintained during transcription mediated by the chromatin remodeler RSC and histone chaperone NAP1 in vitro, Proc. Natl. Acad. Sci. USA 109 (2012) 1931–1936.
[23] A.J. Cook, Z.A. Gurard-Levin, I. Vassias, G. Almouzni, A specific function for the histone chaperone NASP to fine-tune a reservoir of soluble H3-H4 in the histone supply chain, Mol. Cell 44 (2011) 918–927.
[24] C. Warren, D. Shechter, Fly fishing for histones: catch and release by histone chaperone intrinsically disordered regions and acidic stretches, J. Mol. Biol. 429 (2017) 2401–2426.
[25] B. Zhao, Y. Mei, M.J. Schipma, E.W. Roth, R. Bleher, J.Z. Rappoport, A. Wickrema, J. Yang, P. Ji, Nuclear condensation during mouse erythropoiesis requires caspase-3-mediated nuclear opening, Dev. Cell 36 (2016) 498–510.
[26] M.A. Reilly, B. Rapp, P.D. Hamilton, A.Q. Shen, N. Ravi, Material characterization of porcine lenticular soluble proteins, Biomacromolecules 9 (2008) 1519–1526.
[27] J.E. Ladbury, G. Klebe, E. Freire, Adding calorimetric data to decision making in lead discovery: a hot tip, Nat. Rev. Drug Discov. 9 (2010) 23–27.
[28] P.J. Muchowski, L.G. Hays, J.R. Yates 3rd, J.I. Clark, ATP and the core "alpha-Crystallin" domain of the small heat-shock protein alphaB-crystallin, J. Biol. Chem. 274 (1999) 30190–30195.